



Free radicals-triggered reductive and oxidative degradation of highly chlorinated compounds via regulation of heat-activated persulfate by low-molecular-weight organic acids

Jianhua Qu^a, Xue Tian^a, Xiubo Zhang^a, Jiayi Yao^b, Jiaqi Xue^a, Kaige Li^a, Bo Zhang^a, Lei Wang^a, Ying Zhang^{a,*}

^a School of Resources and Environment, Northeast Agricultural University, Harbin 150030, China

^b School of Urban and Environmental Sciences, Key Laboratory of the Ministry of Education for Earth Surface Processes, Peking University, Beijing 100871, China

ARTICLE INFO

Keywords:

Persulfate
Reductive radicals
Degradation
Chlorinated compounds
Chemical oxidation

ABSTRACT

Heat/persulfate (PS)-based chemical oxidation for soil and groundwater remediation is limited in its ability to degrade highly chlorinated compounds (HCCs) due to their insensitivities to electrophilic radicals (e.g. $\text{SO}_4^{\bullet-}$ and $\cdot\text{OH}$). Herein, we developed a universal system for reductive radicals formation with nucleophilic character through hydrogen atom transfer between low-molecular-weight organic acids (LMWOAs) and electrophilic radicals. Specifically, we found that oxalic acid could regulate heat/PS system to generate carbon dioxide radical anion ($\text{CO}_2^{\bullet-}$) which initiated nucleophilic reduction of dichlorodiphenyltrichloroethane (DDT), followed by $\text{SO}_4^{\bullet-}/\cdot\text{OH}$ -initiating electrophilic oxidization of dechlorination intermediates. The $\text{CO}_2^{\bullet-}$ was oxygen-dependent, resulting in higher DDT degradation performance in anaerobic environment, and corresponding degradation pathways were elucidated by theory calculations. Most importantly, compared to heat/PS system, appropriately distributing the amount of $\text{CO}_2^{\bullet-}$ and $\text{SO}_4^{\bullet-}/\cdot\text{OH}$ by regulating additive concentration of oxalic acid significantly increased degradation efficiency (32.34%), degradation rate (174.20%), and mineralization efficiency (29.57%) on DDT, revealing great potentials of proposed system.

1. Introduction

Chlorinated organic compounds are extensively employed in chemical synthesis (e.g. pesticides and organic solvents), which are poisonous and hard-to-biodegrade due to the existence of chlorine atoms [1]. Especially, highly chlorinated compounds (HCCs) are highly oxidized and always possess strong toxicity, environmental persistence and bioaccumulation, seriously threatening ecological environment security and human health [2]. Taking dichlorodiphenyltrichloroethane (DDT) as an example, although it has been gradually banned since 1982, the concentrations of DDT contained in 1.9% of soil specimens from China have been reported to exceed regulatory value (1 mg/kg) [3].

Recently, various techniques have been developed for organic pollutants removal, such as adsorption [4], biodegradation [5], and in situ chemical oxidation (ISCO), among which ISCO has attracted extensive attentions [6]. ISCO relates to introduction of oxidants to soil or groundwater with assistance of activation methods for producing

oxidative free radicals (OFRs) such as $\text{SO}_4^{\bullet-}$ and $\cdot\text{OH}$ to contaminants degradation [7]. Compared to conventional oxidants, persulfate (PS) as an emerging strong oxidant possesses more stability with easier migration in subsurface environment [8,9]. Multiple approaches can be employed for PS activation, for instance, transition metals [10], ultrasonic [11], microwave [12], and carbon materials [13], of which heat activated PS as a clean method has received extensive attentions owing to its easy operation and cost-effectiveness [14], thus making heat/PS-based ISCO technologies more appropriate for contaminated sites remediation. However, corresponding degradation performance of HCCs by heat/PS system is extremely limited, for instance, only 11% of hexachloroethane (1 μM) could be degraded within 60 min by heat activated PS at 50 °C [15]. Moreover, it needed 60 h to achieve 96% of CCl_4 (1 mM) degradation at PS concentrations up to 500 mM at 50 °C of heat/PS system [16]. Additionally, α -hexachlorocyclohexanes (α -HCH) and β -HCH (HCHs=358 mg/kg) in soil could be degraded by 55% and 45%, respectively, after 13 d reaction in the heat/PS system at 45 °C

* Corresponding author.

E-mail address: zhangying_neau@163.com (Y. Zhang).



[17]. This is related to the fact that $\text{SO}_4^{\bullet-}$ and $\cdot\text{OH}$ with electrophilic characters tend to attack electron-rich groups, whereas the carbon chains of HCCs lack electrons due to electron-absorbing action of chlorine atoms, thus leading to severely low reactivities between HCCs and OFRs [18,19].

Considering that HCCs are recalcitrant to oxidative degradation but easily undergo reductive degradation, multiple attentions were paid on PS-based production of reductive free radicals (RFRs). Previous studies have identified that reductive persulfate radicals ($\text{S}_2\text{O}_8^{\bullet-}$) could be generated under anaerobic conditions through electron transfer process between $\text{SO}_4^{\bullet-}/\cdot\text{OH}$ and PS [15]. While the formed amount of $\text{S}_2\text{O}_8^{\bullet-}$ could not be effectively controlled due to its further interaction with PS for $\text{SO}_4^{\bullet-}$ formation, which might affect the reductive degradation efficiency. Moreover, there were reports showing that $\text{SO}_4^{\bullet-}/\cdot\text{OH}$ could react with soil organic matter (SOM) to produce reductive alkyl-like radicals (R^{\bullet}), whereas the reductive degradation performance was dependent on the SOM content [20]. In addition, recent works revealed that ethanol could interact with $\text{SO}_4^{\bullet-}/\cdot\text{OH}$ via H-abstraction and electron transfer pathways to generate reductive ethanol radicals, however, ethanol is volatile substance and the generated alcohol radicals ($\cdot\text{CH}(\text{CH}_3)\text{OH}$) with slightly negative redox potential (E^0) of -1.25 V might exhibit weakly reductive degradation of contaminants [21]. Consequently, it appears essential to explore effective regulation methods on heat/PS system for sustained generation of RFRs with highly negative E^0 value, so as to realize efficiently reductive degradation of HCCs.

As an analog to the molecular structure of ethanol, low-molecular-weight organic acids (LMWOAs) also have active hydrogen atoms [22, 23], and therefore it was hypothesized that LMWOAs can interact with OFRs through H-abstraction for giving rise to RFRs. Moreover, LMWOAs could be viewed as green regulator because they are soluble organic substances that extensively exist in soil environment, and can be used as carbon source for improving activities of soil microorganisms [24]. However, there has been limited work on exploring the influence of LMWOAs on heat-activated PS relating to reductive degradation of HCCs in soil.

On the other hand, although the more amount of chlorine atoms the HCCs possess, the easier it is to reductively degrade them, HCCs are difficult to be completely reduced and the produced dechlorination intermediates are always toxic [25]. As is well known, $\text{SO}_4^{\bullet-}$ and $\cdot\text{OH}$ contribute to mineralization of contaminants in the heat/PS system [26], and thus it is particularly necessary to regulate sequence and amount of RFRs and OFRs generated for effective mineralization of HCCs in soil. Considering that the addition of LMWOAs to heat/PS system may be conducive to RFRs formation, while OFRs can be generated in the absence of LMWOAs, we put forward the hypothesis for high-performance degradation and mineralization of HCCs through two-stage processes, i.e., reductive degradation of HCCs by RFRs generated in the heat/PS/LMWOAs system with subsequent oxidative degradation of dechlorination intermediates by OFRs after the consumption of LMWOAs.

With these hypotheses in mind, DDT as a typical kind of HCCs was selected as model contaminant, and the primary targets were: (1) to identify potential contributions of LMWOAs to heat/PS system for reductive degradation of DDT; (2) to elucidate possible formation pathways and reactive species of RFRs with corresponding degradation pathways of DDT in heat/PS/LMWOAs system by density functional theory (DFT) calculation; (3) to examine DDT degradation and mineralization performance in soil slurry by regulating the generated amount of RFRs and OFRs in heat/PS/LMWOAs system, and to explore the universality of this system for different HCCs degradation.

2. Materials and methods

2.1. Materials

1,1,1-trichloro-2,2-bis(4-chlorophenyl)ethane (p,p'-DDT, >99.9%) was supplied by Dr. Ehrenstorfer GmbH. Sodium persulfate ($\text{Na}_2\text{S}_2\text{O}_8$, 99%), acetone, potassium dichromate, humic acid, n-hexane, trichloroethylene, tetrachloromethane, hexachloroethane, chlordane and various LMWOAs including acetic acid, oxalic acid, formic acid, benzoic acid, gallic acid, p-hydroxybenzoic acid, and protocatechuic acid were provided by Tianjin Kermel Chemical Reagents Co., Ltd. The chemicals with analytical grade were employed herein without additional purification. Main properties of used soils were listed in Text S1.

2.2. Experimental design

Degradation experiments in aqueous phase were conducted in brown serum bottles of 25 mL volume capped by PTFE caps. The total reaction solution volume was fixed to 10 mL containing 28 μM DDT, 10 mM PS and appropriate concentrations of LMWOAs, and the serum vials were then positioned in heatable reciprocating oscillator at 50 °C for initiating the reaction. For anaerobic degradation, the mixed solution was blown for 30 min using nitrogen prior to degradation process. Control experiments without addition of LMWOAs were conducted in parallel. The samples taken at predetermined time intervals were instantly set in iced water (0 °C) to stop the reaction, thereafter, 5 mL of hexane was added to extract DDT for gas chromatography (GC) analysis.

Experiments on soil remediation were carried out in brown serum vials (25 mL) with Teflon caps. 1 g of DDT-polluted soil (10 mg/kg), 5 mL of reaction mixture containing PS (10 mg/kg), and certain amount of LMWOAs were added to the bottles. As to anaerobic remediation studies, deionized water was cleared for 30 min by nitrogen, and then added to the system. The incubation was performed on a rotatory shaker with the temperature maintaining at 50 °C for 72 h. At each sampling time, the reaction was quenched by iced water and the suspension was centrifuged with the discarding of supernatant and vacuum freeze-drying of soil slurry. Subsequently, 5 mL of equal-volume hexane and acetone was added to the bottles with 1 h of ultrasonic treatment for DDT extraction and GC analysis.

2.3. Analytical methods

GC (Shimadzu 2014 C, Japan) containing electron capture detection was employed for identifying DDT concentration in solvent. Chromatographic separation was accomplished using HP-5 column at nitrogen condition (1.0 mL/min) with 1.0 μL of sample volume. Temperatures associating to injector/detector were 215/300 °C. The method for determining the concentrations of DDD/DDE was similar to that of DDT. The concentrations of extracted DDT from soil were determined by shunt injection with a shunt ratio of 4:1. Moreover, the degradation products of DDT were identified using GC-MS (Agilent 7890A-7000B, USA).

The EPR spectra were acquired by JEOL FA300 Bruker ELEXSYS-II (E500 CW-EPR) with 9.05 GHz and 100 kHz of resonance and modulation frequencies, 60 s of sweep interval, and 65536 dB of reception. For each sample vial, 100 mM DMPO was added as the spin-trap agent with reaction for 5 min. The concentrations of chloride ions generated were analyzed by ion chromatography (ICS 930, metrohm). DDT decomposition pathways were analyzed via DFT calculation conducted by CASTEP and Dmol3 modules in materials studio (Text S2). Moreover, quantitative structure-activity relationship (QSAR) estimation was applied to toxicity assessment of DDT degradation intermediates (Text S3).

3. Results and discussion

3.1. Influence of LMWOAs on reductive DDT degradation in aqueous phase

During heat activation of PS, it was found that only 67.65% of DDT was removed from aqueous phase after 240 min, while the DDT degradation was significantly elevated in the presence of LMWOAs such as lower fatty acids (e.g. formic/acetic/oxalic acids) and aromatic organic acids (e.g. benzoic/p-hydroxybenzoic/protocatechuic/gallic acids), as shown in Fig. 1a-b. Furthermore, the universal promotions of LMWOAs on heat activated PS for DDT degradation were identified by increasing LMWOAs concentrations from 2 to 5 mM (Figs. S1a-f), especially for oxalic acid (OA) (Fig. 1c). However, total organic carbon (TOC) was found to decrease only by 5.3% within 240 min after the addition of 5 mM oxalic acid to the heat/PS system (Fig. S2). Thus, we hypothesized that during the interactions between LMWOAs and $\text{SO}_4^{\bullet-}$ /•OH in the heat/PS system, certain types of RFRs were formed for reductive degradation of DDT, and significantly affected the following oxidization and mineralization of intermediates.

3.2. Reactive species formation and identification

3.2.1. Free radical quenching investigations

$\text{K}_2\text{Cr}_2\text{O}_7$ was first chosen as electron scavenger [27], in order to evaluate the role of RFRs in the heat/PS/OA system (Fig. 2a). As observed, the addition of 1 mM Cr(VI) presented significant restraining effect on DDT decomposition in aqueous phase within 45 min, whereas the degradation was not completely impeded due to insufficient amount of Cr(VI), thus leading to fast DDT degradation during the subsequent reaction process. As expected, the DDT degradation efficiency by heat/PS/OA system distinctly declined from 97.87% to 38.98% and 22.47% with the existence of 5 and 10 mM Cr(VI), respectively. Furthermore, it was found that the DDT degradation performance in

heat/PS system was obviously superior to that of heat/PS/OA system under 10 mM Cr(VI). The possible reason was that oxalic acid fiercely inhibited production of $\text{SO}_4^{\bullet-}$ and •OH by reacting with these OFRs to form RFRs, the reductive role of which was subsequently quenched by abundant Cr(VI), thus resulting in deteriorative degradation. In addition, CCl_4 was used as RFRs probe to conduct the degradation test, as shown in Fig. S3. The results showed that the degradation efficiency of CCl_4 in the heat/PS system was only 24.10% within 240 min, while the degradation efficiency of CCl_4 in the anaerobic heat/PS/OA system increased to 67.02%. This further demonstrated the generation of RFRs in the anaerobic heat/PS/OA system.

As is well known, $\text{SO}_4^{\bullet-}$ and •OH are dominant active species during heat activation of PS, and $\text{SO}_4^{\bullet-}$ is the source of •OH [28,29]. Consequently, scavengers of phenol and tert-butanol (TBA) were further employed to assess $\text{SO}_4^{\bullet-}$ function in RFRs formation and DDT degradation [30]. As presented in Fig. 2b, the DDT degradation efficiency in the heat/PS/OA system decreased to 98.98%, 98.30%, 93.52%, 82.44%, and 66.14% with the existence of 1, 5, 10, 50, and 100 mM TBA, respectively. It was well known that the reaction rate of $\text{SO}_4^{\bullet-}$ and TBA was slow ($(4\text{--}9.1)\times 10^5 \text{ M}^{-1} \text{ s}^{-1}$), thus leading to slight inhibition on RFRs formation under low concentration of TBA [30]. Whereas, due to superior interaction between phenol and $\text{SO}_4^{\bullet-}$ ($8.8\times 10^9 \text{ M}^{-1} \text{ s}^{-1}$) [31], the RFRs formation was severely restrained even under low phenol concentration (Fig. 2c), specifically, the removal efficiency distinctly declined to 53.24%, 50.12%, and 18.29% after the addition of 1, 5, and 10 mM phenol, respectively. Overall, the reductive dechlorination of DDT by RFRs has been demonstrated as predominant pathway in heat/PS/OA system, and $\text{SO}_4^{\bullet-}$ /•OH participated in the generation of RFRs.

3.2.2. EPR studies

The formation and species of RFRs in the heat/PS/OA system were further identified by EPR techniques. From Fig. 2d, the DMPO-OH signal was found to be dominant during heat activated PS process, while the

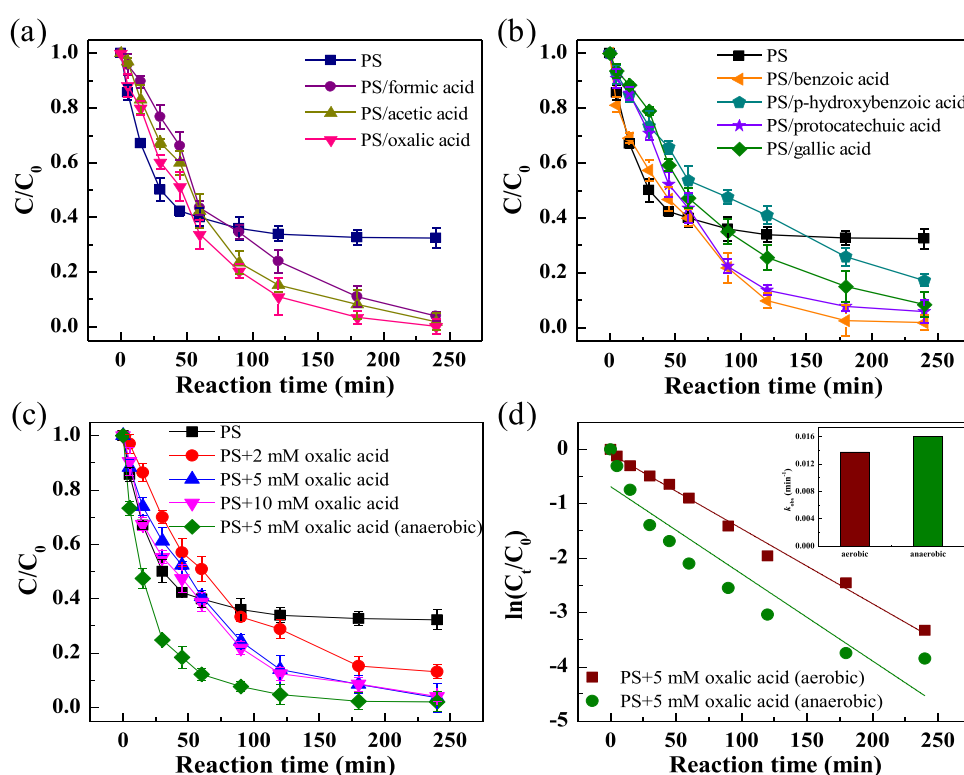


Fig. 1. (a) and (b) Comparisons of DDT degradation performances by different heat/PS/LMWOAs systems; (c) effects of different oxalic acid concentrations on heat/PS system for DDT decomposition. [General conditions: [DDT] = 28 μM , [PS] = 10 mM, T = 50 °C, reaction time = 240 min, pH = 3.75].

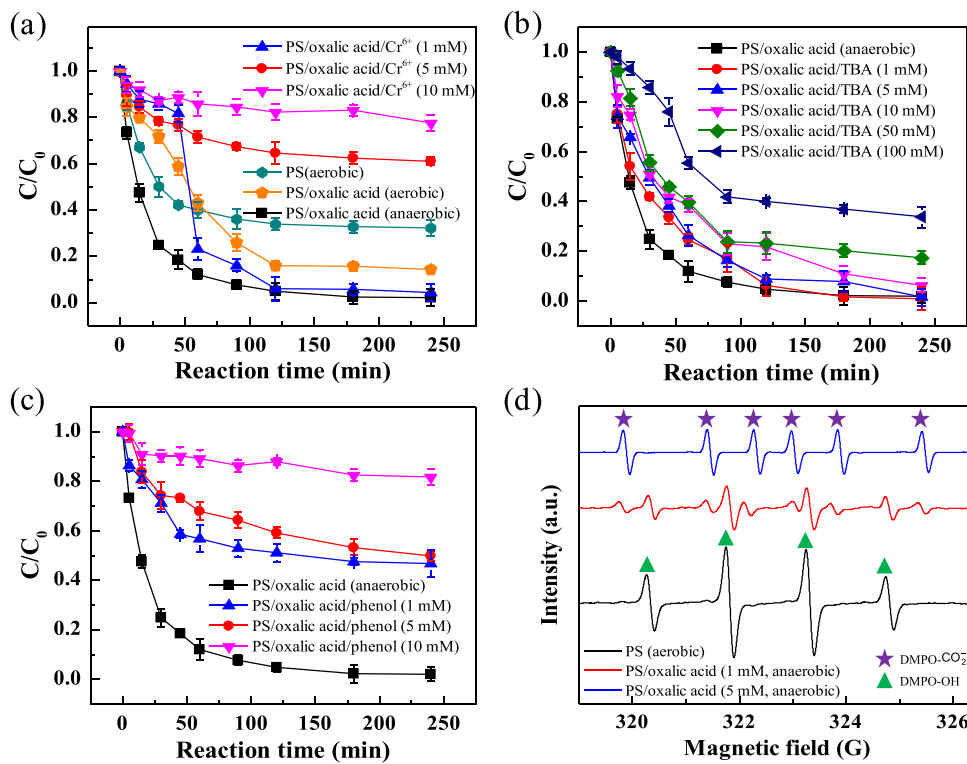
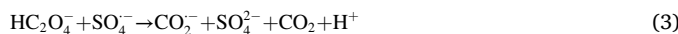


Fig. 2. Influences of different concentrations of (a) Cr(VI), (b) TBA, and (c) phenol on DDT decomposition in the heat/PS/OA system; (d) EPR spectra of free radicals generation in aerobic heat/PS system and anaerobic heat/PS/OA system. [General conditions: [DDT] = 28 μ M, [PS] = 10 mM, T = 50 °C, reaction time = 240 min, pH = 3.75. Specific conditions for (d) [DMPO] = 100 mM, reaction time = 5 min].

signal of DMPO-SO₄ was inconspicuous, which was possibly ascribed to superior interaction between DMPO and •OH [32]. However, after the addition of 1 mM oxalic acid into the system, the DMPO-OH intensity fell by 58.70% with identification of another signal possessing intensity of 1:1:1:1:1, which could be assigned to DMPO-CO₂⁻ [33,34]. This indicated that carbon dioxide radical anion equivalent to CO₂⁻ was generated in oxalic acid-regulating heat/PS system, and we postulated the formation pathways of CO₂⁻ as follows:



Given the combination of nucleophilic character of CO₂⁻ with highly negative E° value of -2.2 V [35], CO₂⁻ could be viewed as a high-performance type of RFRs for reductive degradation of DDT. By further increasing the oxalic acid concentration to 5 mM, the intensity of DMPO-CO₂⁻ signal obviously increased by 73.75%, while the DMPO-OH signal was insignificant, which might be due to the quenching of •OH by abundant oxalic acid [36]. As shown in Fig. S4, the oxalic acid concentration decreased from 4.92 to 3.13 mM after 240 min of reaction, which further proved that oxalic acid reacted with SO₄²⁻/•OH in the heat/PS/OA system to generate CO₂⁻. The aforementioned analyses confirmed that CO₂⁻ was generated from the heat/PS/OA system, and the amount ratio of CO₂⁻ to •OH/SO₄²⁻ could be effectively controlled by regulating the oxalic acid concentration.

3.3. Reductive and oxidative degradation products of DDT

3.3.1. Cl⁻ release exploration

The released Cl⁻ during DDT degradation in anaerobic heat/PS/OA system was examined for identifying the reductive dechlorination role of

CO₂⁻. As noticed from Fig. 3a, the concentration of generated Cl⁻ was increased as the DDT degradation proceeded. And corresponding pseudo-zero-order rate constants (k_{obs}) were calculated as 6.90×10^{-5} and 6.31×10^{-5} mM/min (Fig. 3b), respectively, demonstrating the dechlorination process of DDT accompanied by Cl⁻ release. Further from Fig. 3c-d, DDE and DDD were identified as primary dechlorination products of DDT, the total concentrations of which in aerobic heat/PS and heat/PS/OA systems were 3.66 and 9.65 μ M, while were 8.48 and 20.44 μ M under anaerobic circumstances, accounting for 21.03%, 93.92%, 93.13%, and 97.03% of DDT degradation within 45 min. Obviously, reductive dechlorination was insignificant in aerobic heat/PS system, while the high accumulation of DDD and DDE in anaerobic system was due to the generated S₂O₈²⁻. Furthermore, reductive dechlorination was confirmed as primary pathway of DDT degradation in both anaerobic and anoxic heat/PS/OA systems. However, the accumulated amount of DDD and DDE under aerobic process was significantly lower than that under anaerobic circumstance, which was probably due to the quenching effect of oxygen on CO₂⁻ (Eq. (4)) [35]. Also from Fig. 2a, the inhibitions on DDT degradation with the existence of oxygen or 1 mM Cr(VI) showed similar trends in the heat/PS/OA system, whereas a further degradation was subsequently observed in aerobic condition due to continuous generation of CO₂⁻ after the consumption of oxygen, revealing that the DDT degradation by heat/PS/OA system was oxygen-dependent.



Interestingly, it was further found from Fig. 3b that the concentration of released Cl⁻ exceeded the degraded DDT concentration after 60 min, implying that the DDT released not just one Cl⁻ or its intermediates went through further dechlorination during the reaction. Meanwhile, rapid decline of DDD and DDE concentrations was identified after 45 min for heat/PS/OA system (Fig. 3d), revealing further degradation of these dechlorination intermediates. Further from Fig. S5, the highest degradation efficiencies of DDD (83.19%) and DDE (75.11%) were observed

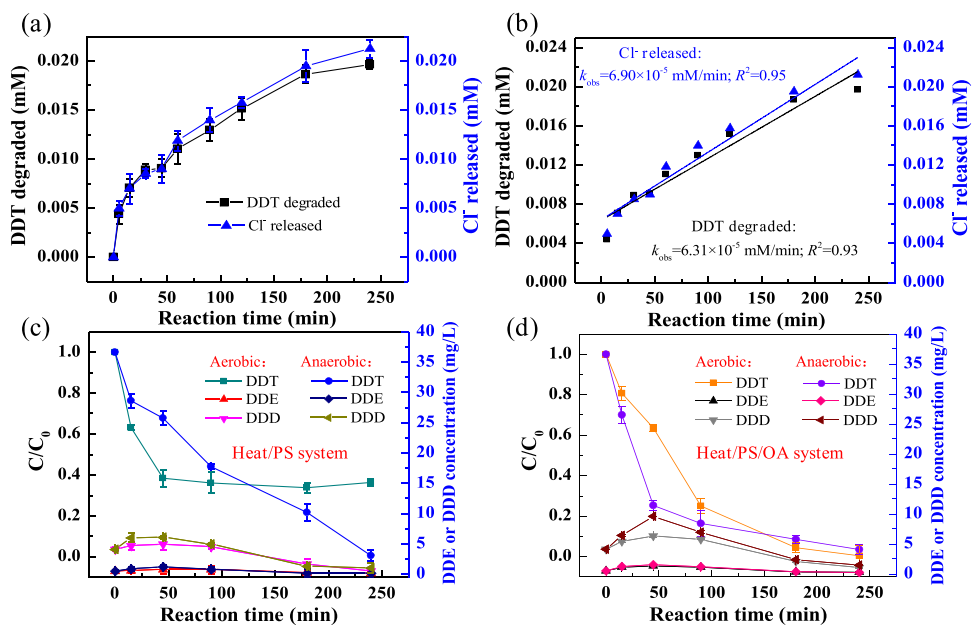
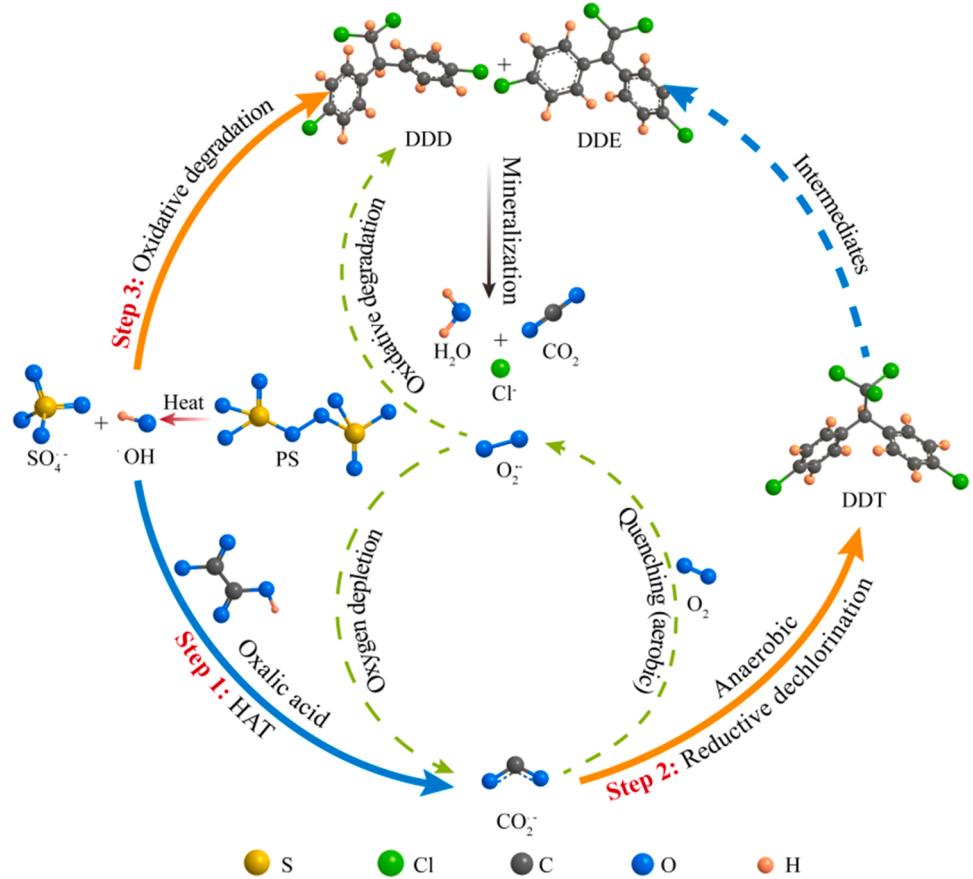


Fig. 3. (a) Quantity of Cl^- released and DDT degraded in anaerobic heat/PS/OA system; (b) plot of k_{obs} of Cl^- release and DDT decomposition; mass balance of DDT degradation by (c) heat/PS and (d) heat/PS/OA systems. [General conditions: [DDT] = 28 μM , [PS] = 10 mM, T = 50 °C, reaction time = 240 min, pH = 3.75].

in the heat/PS system under aerobic circumstance, while only 34.42% of DDD and 51.74% of DDE were eliminated within 240 min in anaerobic heat/PS/OA system, demonstrating excellent affinity of OFRs to such dechlorination intermediates as DDD and DDE.

3.3.2. Proposed pathways of DDT degradation

Considering that DDT is easily degraded via reductive dechlorination, while such dechlorination intermediates as DDD and DDE are more easy to oxidative degradation, we proposed two-step mineralization of DDT by heat activation of PS with existence of proper concentration of



Scheme 1. Proposed reductive dechlorination followed by oxidative degradation mechanisms for DDT decomposition in the heat/PS/OA system.

oxalic acid, i.e., the RFRs of CO_2^- were first employed to reductively degrade DDT, and the OFRs of $\text{SO}_4^{2-}/\text{OH}$ were subsequently generated and applied to oxidative degradation of DDD and DDE after the consumption of oxalic acid, as depicted in Scheme 1.

In term of GC-MS analyses results, a total of 27 kinds of intermediates of DDT were detected, the likely broken bonds positions and active sites of which were elucidated by DFT calculations [36,37]. As observed from Fig. 4b, the C(14)-Cl(3) bond had the smallest Mulliken population value, revealing its easy fracture character [38]. HOMO and LUMO distributions were then employed for estimating possible attacks of electrophilic OFRs and nucleophilic RFRs on DDT molecular [39,40]. From Fig. 4a, the LUMO distribution of DDT showed that the atom of Cl(3) was susceptible to attack by reductive CO_2^- . Meanwhile, the active

sites on DDT were analyzed by Fukui indicators including nucleophilic (f^{+1}), electrophilic (f^{-1}), and radical (f^0) attacks [41]. Notably, the atoms of Cl(1)-Cl(5) possessed relatively higher f^0 values (Fig. 4b), suggesting their more vulnerable characteristics to active species attack, among which the Cl(3) atom was prone to CO_2^- attack because of its largest f^{+1} value, thus resulting in the cleavage of C(14)-Cl(3) with production of DDD (P1) and DDE (P2).

Based on Mulliken population analyses, the bonds of C(14)-Cl(2), C(14)-Cl(1), C(11)-Cl(4), and C(1)-Cl(3) of DDD/DDE were identified to be easier attacked (Figs. S6b and S7b). The HOMO and LUMO distributions of DDD implied that the atoms of Cl(3) and Cl(4) were susceptible to electrophilic attack (Fig. S6a) with the formation of CDPB (P3) and DPB (P6) [40], while the nucleophilic attack was likely to occur on

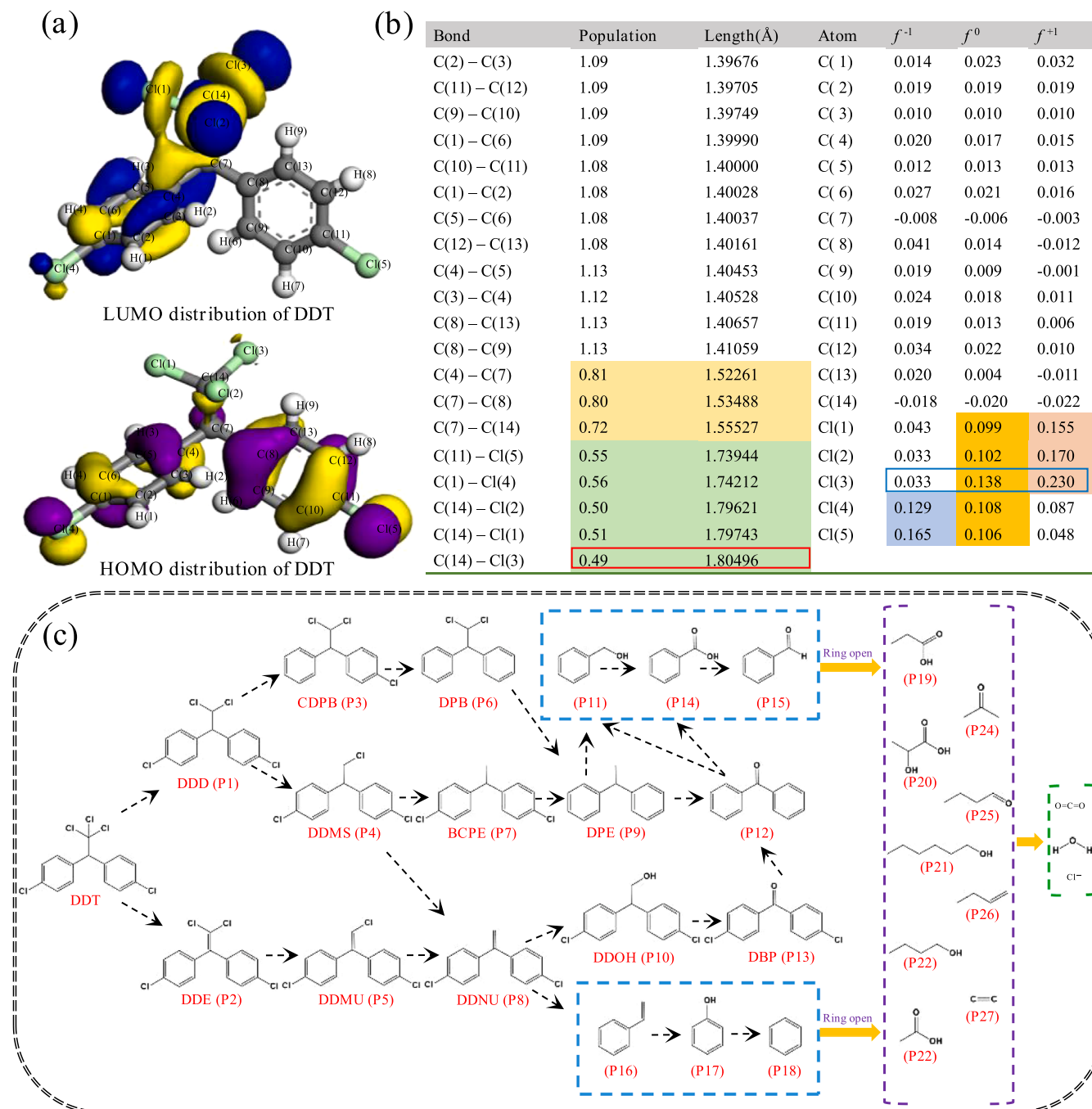


Fig. 4. (a) Locations of HOMO and LUMO orbitals on DDT molecular; (b) the calculated bond orders of DDT molecular and f values of each atom; (c) possible DDT decomposition pathways in the heat/PS/OA system.

Cl(1) and Cl(2) with the generation of DDMS (P4) and BCPE (P7) [42]. Because the total value of the difference between f^{+1} and f^{-1} of Cl(3) and Cl(4) were higher than that of Cl(1) and Cl(2), the electrophilic attack process was identified to be prone to occur on DDD. And then the DDMS could be converted to DDNU (P8) through dehydrochlorination, while the DPB and BCPE could be transformed to DPE (P9) via gradual dechlorination processes. Subsequently, the bond of C(7)-C(8) on DPE with relatively small Mulliken population value was prone to break (Fig. S8), resulting in the generation of P11 and P12 via hydroxylation and oxidation/decarboxylation, respectively. And the bond of C(7)-C(8) on P12 was prone to cleavage with the production of P11 and P14 by addition and hydroxylation reactions, separately (Fig. S9), while P11 could be further oxidized to P14, which was then converted to P15 via dehydroxylation.

As to DDE, the HOMO orbital was mainly located on the four Cl atoms with high f^{-1} values (Fig. S7a-b), suggesting their susceptible characteristics to electrophilic attack with the production of DDMU (P5) and DDNU (P8). It was found from Fig. S10 that the bonds of C(4)-C(7), C(1)-Cl(1), C(11)-Cl(2), and C(7)-C(8) of DDNU with low Mulliken population values were prone to cleavage with the generation of P16, which could be transformed to P17 via consecutive oxidation, decarboxylation, and hydroxylation processes. Subsequently, P18 was finally generated via dehydroxylation of P17. Also, the DDNU could be converted to DDOH (P10) through addition reaction, which was then transformed to P13 via oxidation and decarboxylation processes. As depicted in Fig. S11, the bonds of C(1)-Cl(1) and C(11)-Cl(2) on P13 with low Mulliken population values were prone to attack, resulting in the generation of P12. Through nucleophilic and electrophilic reactions, open-ring processes could subsequently occur on P11 and P14-P18 with the appearance of P19-P27, which were finally mineralized into CO_2 , H_2O , and Cl^- .

Toxicities related to degradation intermediates of DDT were then evaluated by 50% lethal dose value, development toxicity, bioaccumulation factor and mutagenicity through QSAR prediction [42]. As depicted in Text S5, the overall environmental toxicities alleviation of possible intermediates in regard to DDT implied that the heat/PS/OA system could effectively mineralize DDT without generation of more hazardous intermediates.

3.4. Remediation of DDT contaminated soil by distributing RFRs and OFRs in heat/PS/OA system

Reductive degradation effect of CO_2^- on DDT in the soil was first studied. As shown in Fig. 5a, only 39.76% of DDT was eliminated within 72 h by aerobic heat/PS system. However, the decomposition efficiency observably went up to 49.70% and 75.42% with the addition of 5 mM oxalic acid into the system under aerobic and anaerobic circumstances,

respectively, indicating the effective degradation of DDT in the soil by CO_2^- , especially in the absence of oxygen. The variation in oxalic acid concentrations associating with mineralization effectiveness of heat/PS/OA system for DDT in the soil was then investigated. As presented in Fig. 5b, the mineralization efficiency presented by total organic carbon (TOC) soared from 34.80% to 64.37% by increasing the concentration of oxalic acid to 1 mM, which was owing to the incremental number of generated RFRs with the increase of oxalic acid concentration. Nonetheless, obvious inhibition on the mineralization efficiency of DDT (9.14%) was subsequently observed by further increasing oxalic acid concentration to 40 mM. This might be due to that a large number of OFRs were quenched by excessive oxalic acid with less OFRs participating in oxidative degradation of DDD and DDE, thus making these intermediates accumulate without further degradation. And we speculated that in the context of 1 mM oxalic acid, the main reactive species generated from heat/PS/OA system at initial degradation stage were CO_2^- responsible for reductive dechlorination of DDT. While accompanied by gradual depletion of oxalic acid, the quenching influence of oxalic acid on OFRs was weakened with the produced OFRs dominating the system, leading to further oxidative degradation of DDD and DDE. The aforementioned results indicated that the DDT in soil could be effectively mineralized through consecutive reduction dechlorination and oxidation degradation by identifying appropriate additive concentration of oxalic acid in the heat/PS/OA system.

3.5. Effects of operating parameters on DDT degradation in soil

3.5.1. Effect of PS concentration

It was found from Fig. S13a that the DDT degradation efficiency in anaerobic heat/PS/OA system significantly increased from 62.81% to 75.42% at 72 h by increasing PS concentration from 1 to 10 mg/g. The likely reason was that higher concentrations of PS induced the formation of SO_4^-/OH [43], thus contributing to formation of more CO_2^- for promoting reductive degradation of DDT. However, the DDT removal seriously declined to 67.13%, 63.65%, and 58.43% when further increasing PS concentrations to 40, 80, and 160 mg/g, respectively. This was because although continuous increase of PS amount favored generation of more OFRs/RFRs, superabundant PS also consumed large amounts of SO_4^- , thus resulting in a decreased performance in DDT degradation [44].

3.5.2. Effect of temperature

Fig. S13b showed that 63.42–93.87% of DDT was degraded within 72 h with the increase of activation temperature from 40 to 60 °C, demonstrating that the DDT could be efficiently degraded within a wide temperature range. Moreover, the kinetics of DDT removal conformed to pseudo-first-order process, the rate constants of which were identified as

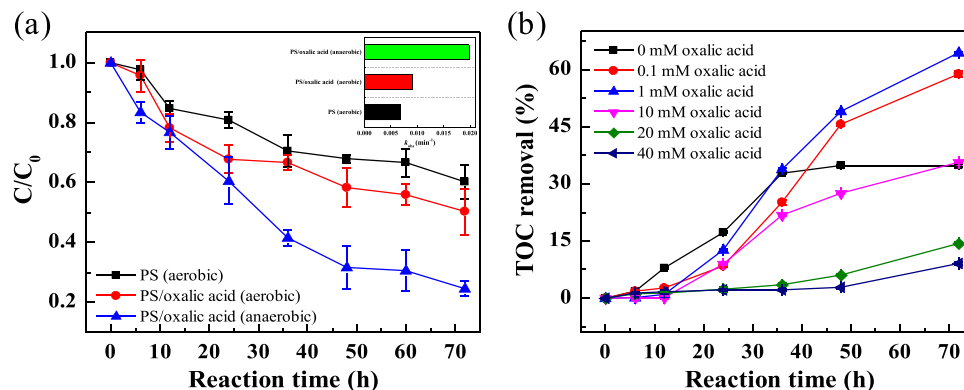


Fig. 5. (a) Kinetics of DDT degradation in soil by heat/PS/OA system with the existence and nonexistence of oxygen; (b) effects of different concentrations of oxalic acid on TOC removal in DDT-contaminated soil by anaerobic heat/PS/OA system. [General conditions: [DDT] = 10 mg/kg, [PS] = 10 mg/g, T = 50 °C, soil: water ratio = 0.2 g/mL, pH = 5.25, reaction time = 72 h. Specific conditions for (a) [oxalic acid] = 5 mM].

0.0087, 0.0096, and 0.0114 min⁻¹, correspondingly. The increasing rate constants were ascribed to the more energy provided by higher activation temperature for cracking PS to accelerate SO₄^{•-}/•OH formation [43], thus leading to generation of more CO₂^{•-} and consequently accounted for DDT degradation with the existence of oxalic acid. Furthermore, the activation energies for DDT elimination by heat-/PS/OA system was calculated as 12.74 kJ/mol via fitting the rate constants by the Arrhenius equation [45], which was markedly lower than that of heat/PS system (43.93 kJ/mol), revealing the facile initiation of the heat/PS/OA system.

3.5.3. Effect of initial soil pH

As observed from Fig. S13c, the DDT degradation efficiency soared from 63.49% to 84.92% with the soil pH increasing from 3.0 to 7.0, revealing that the DDT could be effectively degraded over an extensive pH range in heat/PS/OA system. It is worth noting that at pH ≈ 3, HC₂O₄⁻ occupies above 90% of oxalic acid species because of pK_{a1} (OA) (1.25) and pK_{a2} (OA) (4.28) [34,46]. We also measured the soil pH after the addition of PS and oxalic acid, which was 1.41, 1.92, and 3.35 matching to preliminary soil pH of 3.0, 4.0, and 7.0, respectively. Consequently, the maximized remediation performance was achieved by heat/PS/OA system on the DDT-contaminated soil with initial pH of 7.0, which was owing to the considerable quantity of HC₂O₄⁻. Considering that the soil pH of most HCCs-contaminated sites was during the range of neutral or slightly acidic conditions [3,47], the heat/PS/OA system could be viewed as a superior soil remediation alternative.

3.6. Influences of environmental conditions on DDT degradation in soil

3.6.1. Influence of SOM

SOM is an important component of the soil solid phase, which plays an extremely important role in the remediation of contaminated soil [48,49]. From Fig. S14a, the DDT decomposition efficiency was confirmed to rise from 27.39% to 59.49% during heat-activated PS with SOM content increasing from 20.06 to 61.52 g/kg, which was due to the formation of reductive R[•] from the reactions of OFRs and SOM [20]. Comparatively, after addition of 1 mM oxalic acid in the system, significant increase of DDT degradation efficiency under each SOM content was observed following a gradually upward trend from 75.42% to 88.72%, revealing the synergistical promotions of R[•] and CO₂^{•-} on the reductive degradation of DDT in soil. Furthermore, to avoid variations in physicochemical soil characteristics on DDT degradation, we also carried out the research by adding different concentrations of humic acid in the soil containing SOM of 20.06 g/kg (Fig. S14b), and similar promotion trends were identified further verifying the combined effect of the aforementioned two types of RFRs.

3.6.2. Influence of anions

It is well known that such anions as Cl⁻, CO₃²⁻, HCO₃⁻, and NO₃⁻ exist extensively in soil [50–52], and may exhibit different impacts on DDT degradation in heat/PS/OA system. Fig. S15a showed that the presence of 1–10 mM Cl⁻ presented serious inhibition on DDT degradation, resulting in decreased removal efficiency from 75.42% to 31.19%. The likely reason was that Cl⁻ could react with OFRs and other chloride species to produce Cl[•] and Cl₂^{•-} with relatively lower E° values of 2.6 and 2.3 V (Eqs. (5) and (6)) [53], respectively, in comparison with SO₄^{•-} (E° of 2.5–3.1 V)/•OH (E° of 2.8 V). Interestingly, a further increase of Cl⁻ concentration to 50 mM was found to enhance the DDT degradation efficiency to 88.78%. This might be because that the generated large quantity of Cl[•] could interact with each other for producing active chlorine of Cl₂ with subsequent formation of highly oxidative HClO (Eqs. (7) and (8)) [54], thereby enhancing the catalytic performance.



As observed from Figs. S15b-c, the existence of HCO₃⁻ and CO₃²⁻ had obvious inhibition on DDT removal by heat/PS/OA system, resulting in deteriorative removal efficiency of 41.60% and 27.05% by increasing the HCO₃⁻ and CO₃²⁻ concentrations to 50 mM. This was because that HCO₃⁻ and CO₃²⁻ could compete with DDT and corresponding intermediates for reacting with SO₄^{•-}/•OH to form CO₃²⁻ with remarkably lower E° value of 1.78 V (Eqs. (9)–(11)) [45]. Similarly, NO₃⁻ also presented inhibitory effect by quenching SO₄^{•-}/•OH to produce NO₃[•] with relatively lower E° value of 2.3–2.5 V [55], whereas it was found from Fig. S15d that the DDT degradation efficiency slightly decreased by 8.05% at the presence of 50 mM NO₃⁻, which was most likely due to relatively slower rate of reaction between NO₃⁻ and SO₄^{•-}/•OH than that of HCO₃⁻ and CO₃²⁻ (Eq. (12)) [55].



3.7. Universality evaluation of heat/PS/LMWoAs system

The universality of different types of LMWoAs on the promotions of heat-activated PS for remediation of DDT-polluted soil was examined. As noticed in Figs. S16a-b, compared to heat/PS system, the additions of such lower fatty acids as formic acid and acetic acid could boost DDT degradation efficiencies by 5.60% and 10.82% under aerobic circumstance, while corresponding elevated percentages were 9.00% and 24.32% under anaerobic condition. From Figs. S16c-f, it was found that addition of various aromatic organic acids could also enhance DDT degradation efficiencies by 3.37–14.24% and 16.58–25.19% under aerobic and anaerobic conditions, respectively. On the other hand, four other common HCCs including trichloroethylene (TCE), tetrachloromethane (CCl₄), hexachloroethane (HCA), and chlordane were served as target pollutants for ubiquity assessment of heat/PS/LMWoAs system for degradation of different HCCs. As observed from Fig. 6, the removal efficiencies of TCE, CCl₄, HCA, and chlordane were 85.83%, 77.16%, 54.31%, and 64.58% for aerobic heat/PS/OA system, while were 87.69%, 82.93%, 55.97%, and 77.07% for corresponding anaerobic system, distinctly superior to that of heat-activated PS.

4. Conclusions

Overall, a novel heat/PS/OA system was developed in this study for effective remediation of DDT-contaminated soil and water. Through hydrogen atom transfer between SO₄^{•-}/•OH and oxalic acid, CO₂^{•-} was generated and played a critical role for degradation and mineralization of DDT. Specifically, by adding oxalic acid (1 mM) to conventional heat/PS system, reductive dechlorination of DDT by CO₂^{•-} with oxidative degradation of dechlorination intermediates (e.g. DDD and DDE) by SO₄^{•-}/•OH were sequentially achieved under oxygen-deficient deep subsurface environments. As to shallow surface environments, the reductive degradation of DDT was initially inhibited due to oxygen-sensitive character of CO₂^{•-}, which could contribute to dechlorination of DDT after oxygen depletion. Most importantly, effective regulation of oxalic acid concentration for distributions of CO₂^{•-} and SO₄^{•-}/•OH formed from heat/PS/OA system achieved significantly higher degra-

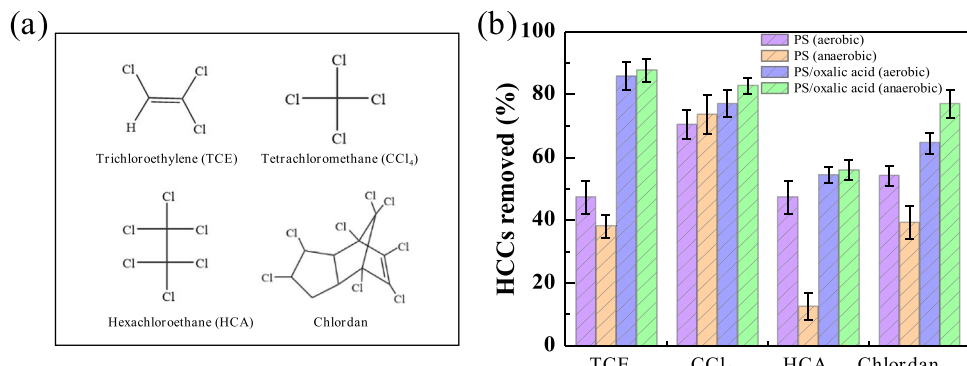


Fig. 6. (a) Chemical structures of TCE, CCl₄, HCA and Chlordane; (b) corresponding HCCs removal efficiencies in soil by heat/PS/OA system under anaerobic conditions. [General reaction conditions: [TCE] = 100 mg/kg, [CCl₄] = 100 mg/kg, [HCA] = 10 mg/kg, [Chlordane] = 10 mg/kg, [PS] = 10 mg/g, [oxalic acid] = 1 mM, reaction time = 72 h, soil-water ratio = 0.2, T = 50 °C, pH = 5.25].

dation and mineralization performances on DDT in the soil, in comparison with heat/PS system. Additionally, the promotion effects of multifarious LMWOAs have been identified, and corresponding heat/PS/LMWOAs systems have great potentials for degradation of various HCCs, thus providing new thoughts to heat/PS-based ISCO for high-performance degradation and mineralization of HCCs under different oxygen statuses.

CRediT authorship contribution statement

Jianhua Qu: Conceptualization, Methodology, Formal analysis, Investigation, Visualization, Writing – original draft. **Xue Tian:** Investigation, Methodology, Writing – review & editing. **Xiubo Zhang:** Formal analysis. **Jiayi Yao:** Investigation. **Jiaqi Xue:** Investigation. **Kaige Li:** Resources. **Bo Zhang:** Writing – review & editing. **Lei Wang:** Writing – review & editing. **Ying Zhang:** Conceptualization, Supervision, Funding acquisition.

Declaration of Competing Interest

The authors declare that they have no known competing financial interests or personal relationships that could have appeared to influence the work reported in this paper.

Acknowledgement

This work was funded by NSF for Distinguished Young Scholars (41625002).

Appendix A. Supporting information

Supplementary data associated with this article can be found in the online version at [doi:10.1016/j.apcatb.2022.121359](https://doi.org/10.1016/j.apcatb.2022.121359).

References

- R. Navon, S. Eldad, K. Mackenzie, F.D. Kopinke, Protection of palladium catalysts for hydrodechlorination of chlorinated organic compounds in wastewaters, *Appl. Catal. B Environ.* 119–120 (2012) 241–247.
- C.M. Dominguez, A. Romero, A. Santos, Selective removal of chlorinated organic compounds from lindane wastes by combination of nonionic surfactant soil flushing and Fenton oxidation, *Chem. Eng. J.* 376 (2019), 120009.
- Y. Chen, A. Juhasz, H. Li, C. Li, L.Q. Ma, X.Y. Cui, The influence of food on the in vivo bioavailability of DDT and its metabolites in soil, *Environ. Sci. Technol.* 54 (2020) 5003–5010.
- J.H. Qu, X.F. Lin, Z.Y. Liu, Y. Liu, Z.Y. Wang, S.Q. Liu, Q.J. Meng, Y. Tao, Q. Hu, Y. Zhang, One-pot synthesis of Ca-based magnetic hydrochar derived from consecutive hydrothermal and pyrolysis processing of bamboo for high-performance scavenging of Pb(II) and tetracycline from water, *Bioresour. Technol.* 343 (2022), 126046.
- C.P. Wang, L. Yu, Z.Y. Zhang, B.L. Wang, H.W. Sun, Tourmaline combined with Phanerochaete chrysosporium to remediate agricultural soil contaminated with PAHs and OCPs, *J. Hazard. Mater.* 264 (2014) 439–448.
- C.H. Yen, K.F. Chen, C.M. Kao, S.H. Liang, T.Y. Chen, Application of persulfate to remediate petroleum hydrocarbon-contaminated soil: feasibility and comparison with common oxidants, *J. Hazard. Mater.* 186 (2011) 2097–2102.
- A. Sitzeraki, B. Petri, M. Crimi, H. Mosbæk, R.L. Siegrist, P.L. Bjerg, In situ chemical oxidation of contaminated soil and groundwater using persulfate: a review, *Crit. Rev. Environ. Sci. Technol.* 40 (2010) 55–91.
- Z.H. Diao, J.C. Jin, M.Y. Zou, H. Liu, J.Q. Qin, X.H. Zhou, W. Qian, P.R. Guo, L. J. Kong, W. Chu, Simultaneous degradation of amoxicillin and norfloxacin by TiO₂@nZVI composites coupling with persulfate: synergistic effect, products and mechanism, *Sep. Purif. Technol.* 278 (2021), 119620.
- F. Pan, X.H. Zhong, D.S. Xia, X.Z. Yin, F. Li, D.Y. Zhao, H.D. Ji, W. Liu, Nanoscale zero-valent iron/persulfate enhanced upflow anaerobic sludge blanket reactor for dye removal: insight into microbial metabolism and microbial community, *Sci. Rep.* 7 (2017) 44626.
- S.L. Nimai, H. Zhang, Z.L. Wu, N.W. Li, B. Lai, Efficient degradation of sulfamethoxazole by acetylene black activated peroxydisulfate, *Chinese, Chem. Lett.* 31 (2020) 2657–2660.
- Z. Frontistis, Degradation of the nonsteroidal anti-inflammatory drug piroxicam by iron activated persulfate: the role of water matrix and ultrasound synergy, *IJRPH* 15 (2018) 2600.
- L.M. Hu, P. Wang, T.Y. Shen, Q. Wang, X.J. Wang, P. Xu, Q.Z. Zheng, G.S. Zhang, The application of microwaves in sulfate radical-based advanced oxidation processes for environmental remediation: a review, *Sci. Total Environ.* 722 (2020), 137831.
- R.H. Zhang, M.L. Chen, Z.K. Xiong, Y. Guo, B. Lai, Highly efficient degradation of emerging contaminants by magnetic CuO@Fe₃O₄ derived from natural mackinawite (FeS) in the presence of peroxymonosulfate, *Chinese, Chem. Lett.* 33 (2022) 948–952.
- N.A. Head, J.I. Gerhard, A.M. Inglis, A.N. Garcia, A.I.A. Chowdhury, D. A. Reynolds, C.V. de Boer, A. Sidebottom, L.M. Austrins, J. Eimers, D.M. O'Carroll, Field test of electrokinetically-delivered thermally activated persulfate for remediation of chlorinated solvents in clay, *Water Res.* 183 (2020), 116061.
- C.Y. Zhu, F.X. Zhu, C. Liu, N. Chen, D.M. Zhou, G.D. Fang, J. Gao, Reductive hexachloroethane degradation by S₂O₈²⁻ with thermal activation of persulfate under anaerobic conditions, *Environ. Sci. Technol.* 52 (2018) 8548–8557.
- M.H. Xu, X.G. Gu, S.G. Lu, Z.F. Qiu, Q. Sui, Z.W. Miao, X.K. Zang, X.L. Wu, Degradation of carbon tetrachloride in aqueous solution in the thermally activated persulfate system, *J. Hazard. Mater.* 286 (2015) 7–14.
- C.M. Dominguez, A. Checa-Fernandez, A. Romero, A. Santos, Degradation of HCHs by thermally activated persulfate in soil system: effect of temperature and oxidant concentration, *J. Environ. Chem. Eng.* 9 (2021), 105668.
- F. Minisci, A. Citterio, C. Giordano, Electron-transfer processes: peroxydisulfate, a useful and versatile reagent in organic chemistry, *Acc. Chem. Res.* 16 (1983) 27–32.
- Y. Yang, J.J. Pignatello, J. Ma, W.A. Mitch, Comparison of halide impacts on the efficiency of contaminant degradation by sulfate and hydroxyl radical-based advanced oxidation processes (AOPs), *Environ. Sci. Technol.* 48 (2014) 2344–2351.
- G.D. Fang, X.D. Chen, W.H. Wu, C. Liu, D.D. Dionysiou, T.T. Fan, Y.J. Wang, C. Y. Zhu, D.M. Zhou, Mechanisms of interaction between persulfate and soil constituents: activation, free radical formation, conversion, and identification, *Environ. Sci. Technol.* 52 (2018) 14352–14361.
- S.S. Yang, Z.Y. Huang, P.X. Wu, Y.H. Li, X.B. Dong, C.Q. Li, N.Y. Zhu, X.D. Duan, D. D. Dionysiou, Rapid removal of tetrabromobisphenol A by α -Fe₂O_{3-x}@Graphene@Montmorillonite catalyst with oxygen vacancies through peroxymonosulfate activation: Role of halogen and α -hydroxyalkyl radicals, *Appl. Catal. B: Environ.* 260 (2020), 118129.

[22] I. Gandarias, J. Requieres, P.L. Arias, U. Armbruster, A. Martin, Liquid-phase glycerol hydrogenolysis by formic acid over Ni-Cu/Al₂O₃ catalysts, *J. Catal.* 290 (2012) 79–89.

[23] D.L. Yuan, C. Zhang, S.F. Tang, X. Li, J.C. Tang, Y.D. Rao, Z.B. Wang, Q.R. Zhang, Enhancing CaO₂ fenton-like process by Fe(II)-oxalic acid complexation for organic wastewater treatment, *Water Res.* 163 (2019), 114861.

[24] L. Zhang, X.J. Li, W.L. Zuo, S. Li, G.Z. Sun, W.D. Wang, Y.D. Yu, H. Huang, Root exuded low-molecular-weight organic acids affected the phenanthrene degrader differently: a multi-omics study, *J. Hazard. Mater.* 414 (2021), 125367.

[25] A.N. Garcia, H.K. Boparai, A.I.A. Chowdhury, C.V. de Boer, C.M.D. Kocur, E. Passeport, B.S. Lollar, L.M. Austrins, J. Herrera, D.M. O'Carroll, Sulfidated nano zerovalent iron (S-nZVI) for in situ treatment of chlorinated solvents: a field study, *Water Res.* 174 (2020), 115594.

[26] L.M. Hu, G.S. Zhang, Q. Wang, X.J. Wang, P. Wang, Effect of microwave heating on persulfate activation for rapid degradation and mineralization of p-nitrophenol, *ACS Sustain. Chem. Eng.* 7 (2019) 11662–11671.

[27] T. Li, Y.W. Gao, L.L. Zhang, X.C. Xing, X. Huang, F. Li, Y. Jin, C. Hu, Enhanced Cr (VI) reduction by direct transfer of photo-generated electrons to Cr 3d orbitals in CrO₄²⁻-intercalated BiOBr with exposed (110) facets, *J. Environ. Manag.* 277 (2021), 111386.

[28] H.S. Kan, T.C. Wang, J.X. Yu, G.G. Qu, P. Zhang, H.Z. Jia, H.W. Sun, Remediation of organophosphorus pesticide polluted soil using persulfate oxidation activated by microwave, *J. Hazard. Mater.* 401 (2021), 123361.

[29] Y.U. Shin, E.T. Yun, J. Kim, H. Lee, S. Hong, J. Lee, Electrochemical oxidation-membrane distillation hybrid process: utilizing electric resistance heating for distillation and membrane defouling through thermal activation of anodically formed persulfate, *Environ. Sci. Technol.* 54 (2020) 1867–1877.

[30] C. Liang, H.W. Su, Identification of sulfate and hydroxyl radicals in thermally activated persulfate, *Ind. Eng. Chem. Res.* 48 (2009) 5558–5562.

[31] Z.W. Cheng, J.J. Wang, D.Z. Chen, J.M. Chen, L.N. Wang, J.X. Ye, J.M. Yu, Thermally activated persulfate for gaseous p-xylene removal: process optimization, mechanism investigation, and pathway analysis, *Chem. Eng. J.* 421 (2021), 127728.

[32] X.H. Lu, J.N. Zhao, Q. Wang, D. Wang, H.D. Xu, J. Ma, W. Qiu, T. Hu, Sonolytic degradation of bisphenol S: effect of dissolved oxygen and peroxydisulfate, oxidation products and acute toxicity, *Water Res.* 165 (2019), 114969.

[33] Q. Zhou, W.Y. Niu, Y. Li, X.J. Li, Photoinduced Fenton-simulated reduction system based on iron cycle and carbon dioxide radicals production for rapid removal of Cr (VI) from wastewater, *J. Clean. Prod.* 258 (2020), 120790.

[34] Y. AlSalka, O. Al-Madanat, M. Curti, A. Hakki, D.W. Bahnemann, Photocatalytic H₂ evolution from oxalic acid: effect of cocatalysts and carbon dioxide radical anion on the surface charge transfer mechanisms, *ACS Appl. Energy Mater.* 3 (2020) 6678–6691.

[35] C.M. Hendy, G.C. Smith, Z.H. Xu, T.Q. Lian, N.T. Jui, Radical chain reduction via carbon dioxide radical anion (CO₂^{•-}), *J. Am. Chem. Soc.* 143 (2021) 8987–8992.

[36] B. Delley, An all-electron numerical method for solving the local density functional for polyatomic molecules, *J. Chem. Phys.* 92 (1990) 508–517.

[37] J.H. Lai, X.Y. Jiang, M. Zhao, S.H. Cui, J. Yang, Y.F. Li, Thickness-dependent layered BiOIO₃ modified with carbon quantum dots for photodegradation of bisphenol A: mechanism, pathways and DFT calculation, *Appl. Catal. B: Environ.* 298 (2021), 120622.

[38] P. Xu, P. Wang, Q. Wang, R. Wei, Y. Li, Y.J. Xin, T. Zheng, L.M. Hu, X.J. Wang, G. S. Zhang, Facile synthesis of Ag₂O/ZnO/rGO heterojunction with enhanced photocatalytic activity under simulated solar light: kinetics and mechanism, *J. Hazard. Mater.* 403 (2021), 124011.

[39] S.X. He, R.L. Yin, Y.X. Chen, T.Y. Lai, W.Q. Guo, L.X. Zeng, M.S. Zhu, Consolidated 3D Co₃Mn-layered double hydroxide aerogel for photo-assisted peroxyomonosulfate activation in metronidazole degradation, *Chem. Eng. J.* 423 (2021), 130172.

[40] C. Foroutan-Nejad, A double bond with weak σ - and strong π -interactions is still a double bond, *Nat. Commun.* 12 (2021) 4037.

[41] M.E. Casida, C. Jamorski, K.C. Casida, D.R. Salahub, Molecular excitation energies to high-lying bound states from timedependent density-functional response theory: characterization and correction of the time-dependent local density approximation ionization threshold, *J. Chem. Phys.* 108 (1998) 4439–4449.

[42] S.S. Xin, B.R. Ma, C.L. Zhang, X.M. Ma, P. Xu, G.S. Zhang, M.C. Gao, Y.J. Xin, Catalytic activation of peroxydisulfate by alfalfa-derived nitrogen self-doped porous carbon supported CuFeO₂ for nimesulide degradation: performance, mechanism and DFT calculation, *Appl. Catal. B: Environ.* 294 (2021), 120247.

[43] Z.H. Diao, X.R. Xu, D. Jiang, L.J. Kong, Y.X. Sun, Y.X. Hu, Q.W. Hao, H. Chen, Bentonite-supported nanoscale zero-valent iron/persulfate system for the simultaneous removal of Cr(VI) and phenol from aqueous solutions, *Chem. Eng. J.* 302 (2016) 213–222.

[44] L.Y. Liu, C. Yang, W. Tan, Y. Wang, Degradation of Acid red 73 by activated persulfate in a heat/Fe₃O₄@AC system with ultrasound intensification, *ACS Omega* 5 (2020) 13739–13750.

[45] Q. Wang, X.H. Lu, Y. Cao, J. Ma, J. Jiang, X.F. Bai, T. Hu, Degradation of Bisphenol S by heat activated persulfate: kinetics study, transformation pathways and influences of co-existing chemicals, *Chem. Eng. J.* 328 (2017) 236–245.

[46] Y. AlSalka, A. Hakki, M. Fleisch, D.W. Bahnemann, Understanding the degradation pathways of oxalic acid in different photocatalytic systems: towards simultaneous photocatalytic hydrogen evolution, *J. Photochem. Photobiol. A* 366 (2018) 81–90.

[47] D.E. Morrison, B.K. Robertson, M. Alexander, Bioavailability to earthworms of aged DDT, DDE, DDD, and dieldrin in soil, *Environ. Sci. Technol.* 34 (2000) 709–713.

[48] A.L. Teel, F.C. Elloy, R.J. Watts, Persulfate activation during exertion of total oxidant demand, *Chemosphere* 158 (2016) 184–192.

[49] J.H. Qu, Y.H. Yuan, X.M. Zhang, L. Wang, Y. Tao, Z. Jiang, H. Yu, M. Dong, Y. Zhang, Stabilization of lead and cadmium in soil by sulfur-iron functionalized biochar: Performance, mechanisms and microbial community evolution, *J. Hazard. Mater.* 425 (2022), 127876.

[50] Y.K. Liu, Y. Zhang, B.J. Wang, S.Y. Wang, M. Liu, Y.L. Wu, L.L. Lu, H. Ren, H.J. Li, W.B. Dong, A. Qadeer, Degradation of ibuprofen in soil systems by persulfate activated with pyrophosphate chelated Fe(II), *Chem. Eng. J.* 379 (2020), 122145.

[51] J.H. Qu, S.Q. Wei, Y. Liu, X.M. Zhang, Z. Jiang, Y. Tao, G.S. Zhang, B. Zhang, L. Wang, Y. Zhang, Effective lead passivation in soil by bone char/CMC-stabilized FeS composite loading with phosphate-solubilizing bacteria, *J. Hazard. Mater.* 423 (2022), 127043.

[52] J.H. Qu, M. Dong, F.X. Bi, Y. Tao, L. Wang, Z. Jiang, G.S. Zhang, B. Zhang, Y. Zhang, Microwave-assisted one-pot synthesis of β -cyclodextrin modified biochar for stabilization of Cd and Pb in soil, *J. Clean. Prod.* 346 (2022), 131165.

[53] S.Y. Liou, M.C. Dodd, Evaluation of hydroxyl radical and reactive chlorine species generation from the superoxide/hypochlorous acid reaction as the basis for a novel advanced oxidation process, *Water Res.* 200 (2021), 117142.

[54] X. Yu, Z. Bao, J.R. Barker, Free radical reactions involving Cl[•], Cl₂^{-•}, and SO₄²⁻ in the 248 nm photolysis of aqueous solutions containing S₂O₈²⁻ and Cl, *J. Phys. Chem. A* 108 (2004) 295–308.

[55] P. Neta, R.E. Huie, A.B. Ross, Rate constants for reactions of inorganic radicals in aqueous solution, *J. Phys. Chem. Ref. Data* 17 (1988) 1027–1284.